High-harmonic spectroscopy of molecular isomers

M. C. H. Wong,[1] J.-P. Brichta,[1] M. Spanner,[2] S. Patchkovskii,[2] and V. R. Bhardwaj[1,*]

[1]*Department of Physics, University of Ottawa, 150 Louis-Pasteur, Ottawa, Ontario, Canada K1N 6N5*
[2]*National Research Council of Canada, 100 Sussex Drive, Ottawa, Ontario, Canada K1A 0R6*

We demonstrate that high-order-harmonic generation (HHG) spectroscopy can be used to probe stereoisomers of randomly oriented 1,2-dichloroethylene ($C_2H_2Cl_2$) and 2-butene (C_4H_8). The high-harmonic spectra of these isomers are distinguishable over a range of laser intensities and wavelengths. Time-dependent numerical calculations of angle-dependent ionization yields for 1,2-dichloroethylene suggest that the harmonic spectra of molecular isomers reflect differences in their strong-field ionization. The subcycle ionization yields for the *cis* isomer are an order of magnitude higher than those for the *trans* isomer. The sensitivity in discrimination of the harmonic spectra of *cis-* and *trans-* isomers is greater than 8 and 5 for 1,2-dichloroethylene and 2-butene, respectively. We show that HHG spectroscopy cannot differentiate the harmonic spectra of the two enantiomers of the chiral molecule propylene oxide (C_3H_6O).

The arrangement of atoms in a molecule can influence ion energetics, reaction rates, chemical reactions, and light-matter interactions. Molecular isomers are often identified by their rovibrational absorption fingerprint using infrared, Raman, and microwave spectroscopic techniques [1]. Electronic absorption has also been exploited using wavelength-selective ultraviolet multiphoton ionization [2]. However, collisional techniques based on electron and ion impact had varying degrees of success in linking changes in molecular geometry to dynamical processes. In most cases, the isomers produced similar mass spectra [3–6]. Electron scattering from isomers has only recently demonstrated convincing differences in the absolute total cross sections in the low-energy region [7].

High-harmonic generation (HHG) spectroscopy of simple molecular systems has recently evolved as a new tool to probe electron density in the neutral [8,9] and hole dynamics [10] of an ion via harmonic amplitude, phase, and frequency measurements with angstrom spatial [11] and attosecond temporal resolution. In HHG spectroscopy, strong-field ionization launches an electron wave packet adiabatically into the continuum by tunneling. The wave packet is subsequently driven by the oscillating electric field and recombines with the parent ion, thus emitting high-energy radiation [12]. The ionization step transfers the orbital information onto the harmonic spectra and by treating the recolliding electron as a plane wave, the molecular orbital can be reconstructed [8]. However, extending this technique to complex molecular systems can be difficult due to participation of multiple continua and breakdown of the adiabatic and plane-wave approximations [10,13]. It is therefore unknown whether HHG spectroscopy, with its high spatial and temporal precision, can be used as a sensitive tool to probe complex molecular structure and dynamics.

In this Rapid Communication, we demonstrate that HHG spectroscopy can be used to probe stereoisomers of randomly oriented 1,2-dichloroethylene (1,2-DCE, $C_2H_2Cl_2$) and 2-butene (C_4H_8). We show that differences in strong-field ionization of isomers cause the harmonic spectra to be

distinguishable. Theoretically, we find the ionization yields of *cis*-DCE to be ∼8 times higher than that of *trans*-DCE for different wavelengths. Experimentally, the relative ionization probability between the two isomers is reflected in the ratio of their harmonic spectra. Finally, we show that HHG spectroscopy is insensitive to the chirality of an unaligned molecule.

The molecules that we investigated have low ionization potentials (9.62 and 9.58 eV for *cis-* and *trans-*DCE; 9.11 and 9.12 eV for *cis-* and *trans-*2-butene). Therefore, high-harmonic spectra are obtained using long-wavelength light in the range of 1300 to 1800 nm. At long wavelengths the following effects occur: (a) The energy of the recolliding electron scales quadratically with wavelength so the harmonic cutoff can be extended to high photon energies while the laser intensity is kept below or close to the saturation intensity of the molecule as compared to the use of 800 nm light [14]. Harmonics with photon energies greater than 40 to 50 eV are needed to capture molecular and multielectron dynamics [15,16]. (b) Ionization of polyatomic molecules is adiabatic with less fragmentation [17]. (c) High spatial resolution of the HHG spectroscopic method can be achieved, set by the de Broglie wavelength of the recolliding electron. (d) Phase matching for higher-order harmonics is extended and can be achieved at higher pressures since use of lower laser intensities offsets the detrimental effects of the ionized medium [18,19]. (e) The electron spends more time in the continuum, resulting in large transverse spreading of the recolliding electron wave packet. This reduces the recollision probability and, as a consequence, the harmonic signal scales with wavelength as $\lambda^{-5.5}$ [20,21]. To an extent, this limitation is overcome by use of higher pressures.

Wavelength-tunable infrared light pulses of 80 fs were generated at a repetition rate of 100 Hz with a superfluorescence-seeded optical parametric amplifier pumped by 3.5 mJ, 45 fs, 800 nm pulses. The light pulses, whose energies varied from 900 μJ at 1800 nm to 1.3 mJ at 1300 nm, were focused into a differentially pumped gas cell through a 2-mm-thick CaF_2 window by an achromatic lens of focal length 400 mm. The gas cell is 10 mm long with 600 μm apertures. The harmonics, produced in an ensemble of randomly oriented

———————
*ravi.bhardwaj@uottawa.ca

molecules, were dispersed by a flat-field concave grating at grazing incidence onto a microchannel plate detector coupled to a phosphor screen and then imaged by a charge-coupled device camera. The harmonic spectra are obtained under optimal phase-matching conditions by adjusting the position of the laser focus with respect to the pinholes and the absolute pressure inside the gas cell. Typical densities used in the experiments were $(1–3) \times 10^{17}$ cm^{-3}. The vapor pressures of 1,2-DCE and propylene oxide at room temperature were high enough for them to be introduced into the cell without the use of any carrier gas. The chemicals, acquired from Sigma-Aldrich, have purities of 97% for 1,2-DCE, and 99% for 2-butene and propylene oxide. The intensity of the laser beam was altered between 5×10^{13} and 2×10^{14} W/cm^2 using neutral density filters. Intensity calibration was achieved by monitoring the cutoff harmonics from argon and validated by measuring its saturation intensity using a fast ionization gauge [22,23].

Figure 1(a) shows the harmonic spectra for *cis-* and *trans-*DCE obtained with 1800 nm driving laser pulses at an intensity of 1.1×10^{14} W/cm^2. Although the harmonic spectra of the two isomers are distinctly different, both exhibit an amplitude modulation around 40 eV. *cis-*DCE produces significantly more photons in the plateau region while *trans-*DCE produces more photons in the cutoff region. Figure 1(b) shows the ratio of the harmonic spectra for the two isomers. A value of unity corresponds to the harmonic signals being equal. Since the ionization potentials of the two isomers are nearly identical, similar spectra are expected from the semiclassical model of HHG extended to molecules. The harmonic spectra of the isomers are distinct even when different pressures are used, resulting in similar-looking ratios to those in Fig. 1(b) but with different magnitudes. The differences in harmonic spectra
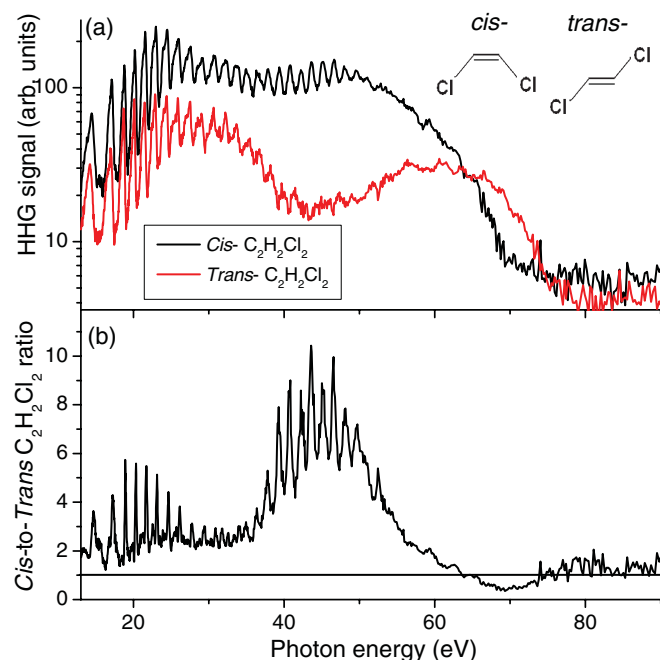
FIG. 1. (Color online) (a) High-harmonic spectra for *cis-* and *trans-*1,2-dichloroethylene obtained using 1800 nm light at an intensity of 1.1×10^{14} W/cm^2. (b) *cis-* to *trans-*1,2-dichloroethylene harmonic ratio of spectra from (a).
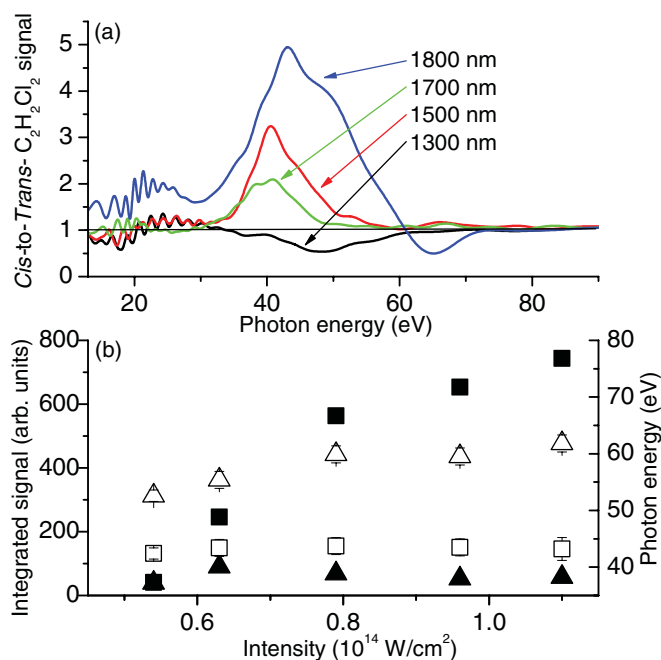
FIG. 2. (Color online) (a) *cis* to *trans* harmonic ratio of 1,2-dichloroethylene for different wavelengths at an intensity of 0.8×10^{14} W/cm^2. (b) Features of the harmonic ratio as a function of intensity using 1800 nm light; ■, the total integrated signal (left scale) of the peak above unity; □, the photon energy (right scale) of the position of the peak above unity; ▲, the total integrated signal of the peak below unity; △, the photon energy (right scale) of the position of the peak below unity.

between the two isomers persist for several wavelengths and over a range of laser intensities.

Figure 2(a) shows the wavelength dependence of the *cis* to *trans* ratio between the harmonic spectra of 1,2-DCE obtained at an intensity of $\sim 8 \times 10^{13}$ W/cm^2. The curves have been smoothed for clarity. At 1300 nm, the two isomers produce similar spectra up to ~ 30 eV. Beyond this energy, the *trans-*DCE signal dominates, producing more high-energy photons up to 55 eV. As the driving wavelength is increased, two things occur. First, the harmonic spectra are extended to higher photon energies; at 1800 nm, photons up to 75 eV are produced. Second, the *cis-*DCE signal starts to dominate at lower photon energies. As the wavelength increases, the position of the peak above unity shifts marginally by ~ 2 eV. The position of the trough, corresponding to the *trans-*DCE signal being dominant, shifts from 50 eV at 1300 nm to 65 eV at 1800 nm.

Figure 2(b) shows the intensity dependence of the integrated signal for the ratio above unity (corresponding to the *cis-*DCE signal being dominant) for 1800 nm light. The signal from *cis-*DCE is greater than that for *trans-*DCE by almost an order of magnitude. The position of the peak above unity does not change with laser intensity. Also shown is the position of the trough below unity (corresponding to the *trans-*DCE signal being dominant) which shifts with laser intensity by ~ 10 eV and is associated with the cutoff harmonics. The integrated signal of the trough below unity does not vary much with intensity.

We now return to the amplitude modulations in the harmonic spectra in Fig. 1(a). The position of the amplitude minimum at ∼40 eV is independent of laser intensity and wavelength (see Fig. 2). Spectral minima of this nature have previously been shown to originate from electronic structure associated with the Cooper minima in the photoionization cross sections of molecules containing chlorine atoms [16,24]. Since recombination is the inverse of photoionization [25], contrast in the harmonic spectra near the Cooper minimum indicates significant difference in the photoionization cross sections of the two isomers.

We calculated the angle-dependent ionization yields using the time-dependent numerical *ab initio* method outlined in [26]. This method uses multielectron quantum chemistry wave functions to represent the multielectron bound states of the neutral atom and cation, and couples these states to Cartesian grids used to represent the continuum states. In the present calculations, we computed the ground state of the neutral and ionic systems using GAMESS [27] with the augmented correlation consistent polarized valence triple-zeta (aug-cc-pVTZ) basis set [28,29] at the Hartree-Fock level. The continuum grid extended to ±15 a.u. in all directions with a grid step size of 0.2 a.u. The time-dependent equations of [26] were integrated using the leapfrog method with a time step of 0.002 66 a.u.

The system is initiated with the whole population in the neutral ground state and then exposed to a half cycle of the carrier oscillations. We use only a half cycle in the calculation of the ionization yield since this is the yield relevant to the subcycle dynamics of the first step in HHG. Further, using only a half cycle allows us to capture the asymmetries in the subcycle ionization yields for the *cis* isomer. We used

absorbing boundaries [30] with a width of 4.3 a.u. at the edges of the continuum grid to prevent reflection of the outgoing electron flux and to calculate the ionization yield by monitoring the population absorbed at the grid edges. The calculation was repeated with several different angles between the molecular axis and the laser polarization direction in order to capture the full angular dependence of the ionization yield.

Figure 3(a) shows the highest occupied molecular orbital (HOMO) of *cis*-DCE and the angular ionization distribution. The HOMO of *cis*-DCE ionizes preferentially when the laser polarization is parallel to the molecular dipole. Figure 3(b) shows the HOMO of *trans*-DCE and the angular ionization distribution. Here the molecule ionizes preferentially along the molecular axis. The half-cycle ionization yields of the two isomers at 800 nm are 10.1% for *cis* and 1.1% for *trans* at an intensity of 1.5×10^{14} W/cm^2. Although ionization yields vary with intensity, the relative differences between the two isomers remain the same. At an intensity of 10^{14} W/cm^2, the yields are 6.6% and 0.8% for 1300 nm and 7.3% and 0.96% for 1500 nm. The ionization yields of *cis*-DCE are ∼7–9 times higher than those of *trans*-DCE. Although we present angular plots for a half-cycle ionization using 800 nm light, calculations for 1300 and 1500 nm distributions show that they look qualitatively similar for all wavelengths considered.

Our experimental results can be interpreted in terms of ionization, the first step in the HHG process. Ionization yields of *cis*-DCE are ∼8 times higher than for *trans*-DCE when 1800 nm light is used. This difference is directly reflected in the ratio of the harmonic spectra of the isomers up to ∼60 eV. Suppression of ionization in *trans*-DCE leads to
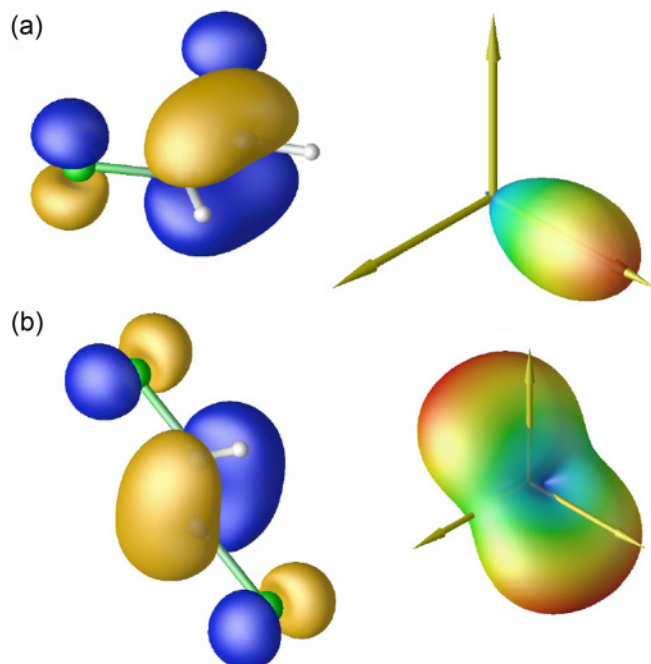

FIG. 3. (Color online) (a) HOMO (left) and angular ionization distribution (right) of (a) *cis* and (b) *trans*-1,2-dichloroethylene. Ionization distributions are calculated at an intensity of 10^{14} W/cm^2 using 800 nm light.
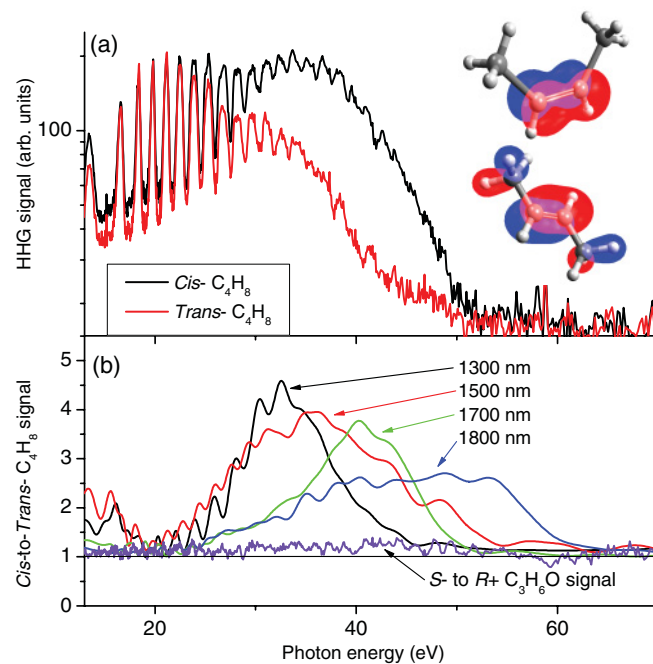

FIG. 4. (Color online) (a) High-harmonic spectra for *cis*- and *trans*-2-butene obtained using 1700 nm light at an intensity of 0.8×10^{14} W/cm^2. (b) *cis*- to *trans*- harmonic ratio of 2-butene at wavelengths 1300–1800 nm at an intensity of 0.9×10^{14} W/cm^2 and the $S-$ to $R+$ harmonic ratio of propylene oxide using 1800 nm light at an intensity of 10^{14} W/cm^2.

extension of the harmonic cutoff, especially when the laser intensity is above saturation [31], and this extension has been observed in simple molecular systems [32]. As a result, *trans*-DCE dominates in the 60 to 75 eV photon energy range (see Fig. 1). When the laser intensity or wavelength is increased, the harmonic cutoff is extended so the peak in the region where *trans*-DCE is dominant shifts to higher energies. Recombination, the final step in the HHG process, can also be influenced by both electronic and molecular structure [9,10,33]. The isomeric effects that we have so far demonstrated are not unique to 1,2-DCE. They should be present in all molecular isomers that differ in their orbital symmetries [34].

Figure 4(a) shows the harmonic spectra for *cis*- and *trans*-2-butene obtained using 1700 nm light at an intensity of 0.8×10^{14} W/cm^2. *Cis*-2-butene is valence isoelectronic to *cis*-DCE. Unlike 1,2-DCE, *cis*-2-butene produces more photons over a range of harmonic energies while *trans*-2-butene is never dominant. Figure 4(b) shows the wavelength dependence of the *cis* to *trans* ratio of the harmonic spectra of 2-butene obtained at an intensity of 0.9×10^{14} W/cm^2. The position of the peak above unity (corresponding to *cis*-2-butene being dominant) shifts to higher energies with increasing wavelength, and the harmonic cutoff extends to higher energies. These results indicate that the relative ionization probabilities of the two isomers differ by a factor of 5. Also shown is the ratio of the harmonic spectra of the left- and right-handed enantiomers of the chiral molecule propylene oxide (C_3H_6O) using 1800 nm light at an intensity of 10^{14} W/cm^2. Both enantiomers produced identical harmonic spectra, resulting in a ratio that is close to unity; an expected result since ionization of unaligned enantiomers should be identical. This outcome is consistent for all wavelengths used (1500–1800 nm) and confirms our interpretation of the isomeric effects.

The ability to distinguish molecular isomers by HHG spectroscopy combined with its high spatial and temporal resolution enables the study of isomerization dynamics. Such a study was recently conducted in the ethylene cation using an extreme-ultraviolet pump and near-infrared probe configuration [35]. The possibility of extracting electronic and molecular structure information from HHG in complex molecules would widen the prospects of using HHG spectroscopy as a sensitive tool to probe not only electron dynamics but also coupled electronic and nuclear dynamics.

[1] E. T. J. Nibbering, H. Fidder, and E. Pines, Annu. Rev. Phys. Chem. **56**, 337 (2005).

[2] J. W. Hudgens, M. Seaver, and J. J. DeCorpo, J. Phys. Chem. **85**, 761 (1981).

[3] J.-Y. Zhang *et al.*, Int. J. Mass Spec. Ion Proc. **110**, 103 (1991).

[4] C. Sottani *et al.*, Org. Mass Spec. **27**, 169 (1992).

[5] V. A. Mikhailov *et al.*, J. Phys. Chem. A **110**, 5760 (2006).

[6] P. Sobocinski *et al.*, J. Phys.: Conf. Ser. **101**, 012006 (2008).

[7] C. Szmytkowski and S. Kwitnewski, J. Phys. B **36**, 4865 (2003).

[8] J. Itatani *et al.*, Nature (London) **432**, 867 (2004).

[9] T. Kanai, S. Minemoto, and H. Sakai, Nature (London) **435**, 470 (2005).

[10] O. Smirnova *et al.*, Nature (London) **460**, 972 (2009).

[11] M. Y. Ivanov and J. P. Marangos, J. Mod. Opt. **54**, 899 (2007).

[12] P. B. Corkum, Phys. Rev. Lett. **71**, 1994 (1993).

[13] W. Li *et al.*, Science **322**, 1207 (2008).

[14] B. Shan and Z. Chang, Phys. Rev. A **65**, 011804(R) (2001).

[15] R. Torres *et al.*, Opt. Express **18**, 3174 (2010).

[16] M. C. H. Wong, J.-P. Brichta, and V. R. Bhardwaj, Phys. Rev. A **81**, 061402(R) (2010).

[17] V. R. Bhardwaj *et al.*, Phys. Rev. Lett. **87**, 253003 (2001).

[18] E. J. Takahashi *et al.*, Phys. Rev. Lett. **101**, 253901 (2008).

[19] T. Popmintchev *et al.*, Opt. Lett. **33**, 2128 (2008).

[20] J. Tate *et al.*, Phys. Rev. Lett. **98**, 013901 (2007).

[21] A. D. Shiner *et al.*, Phys. Rev. Lett. **103**, 073902 (2009).

[22] S. M. Hankin *et al.*, Phys. Rev. A **64**, 013405 (2001).

[23] J.-P. Brichta *et al.*, Phys. Rev. A **79**, 033404 (2009).

[24] T. A. Carlson *et al.*, Z. Phys. D **2**, 309 (1986).

[25] A. D. Shiner *et al.*, Nat. Phys. **7**, 464 (2011).

[26] M. Spanner and S. Patchkovskii, Phys. Rev. A **80**, 063411 (2009).

[27] M. W. Schmidt *et al.*, J. Comput. Chem. **14**, 1347 (1993).

[28] T. H. Dunning Jr., J. Chem. Phys. **90**, 1007 (1989).

[29] D. E. Woon and T. H. Dunning Jr., J. Chem. Phys. **98**, 1358 (1993).

[30] D. E. Manolopoulos, J. Chem. Phys. **117**, 9552 (2002).

[31] Saturation intensity of xenon [ionization potential (IP) ∼12 eV] is ∼10^{14} W/cm^2. For molecules with IP ∼ 9–10 eV the saturation intensity would be ∼5×10^{13} W/cm^2 [22].

[32] B. Shan *et al.*, Phys. Rev. A **66**, 061401(R) (2002).

[33] M. Lein *et al.*, Phys. Rev. A **66**, 023805 (2002).

[34] Unpublished data on the structural isomers butane and isobutane, and 1-propanol and isopropanol.

[35] J. van Tilborg *et al.*, J. Phys.: Conf. Ser. **194**, 012015 (2009).